

ORIGINAL RESEARCH article

Front. Astron. Space Sci., 30 May 2023

Sec. Stellar and Solar Physics

Volume 10 - 2023 | <https://doi.org/10.3389/fspas.2023.1154612>

Download article ▾

2,2K

Total views

392

Downloads

1

Citation

Investigating the variations in the composition and heating of interacting ICMEs

Nandita Srivastava¹Zavkiddin Mirtoshev^{2*}Wageesh Mishra³

¹ Udaipur Solar Observatory, Physical Research Laboratory, Udaipur, India

² Institute of Engineering Physics, Samarkand State University, Samarkand, Uzbekistan

³ Indian Institute of Astrophysics, Bengaluru, India

Share on



Edited by



Divya Oberoi

Tata Institute of Fundamental Research, India

Reviewed by



Emilia Kilpua

We use cookies

Our website uses cookies that are essential for its operation and additional cookies to track performance, or to improve and personalize our services. To manage your cookie preferences, please click Cookie Settings. For more information on how we use cookies, please see our [Cookie Policy](#).

[Cookies Settings](#)[Reject non-essential cookies](#)[Accept cookies](#)

contents

interaction observed in 2012, of which one led to a merged structure after the interaction, as observed at 1 AU. The second interaction event was reported to arrive at L1 as two distinct structures. Our analysis reveals distinct composition signatures in the form of ion charge state enhancements. The results improve our understanding of the signatures of ICMEs and different complex structures formed after the interaction. The study reveals that compression can occur due to the passage of the shock associated with the following CME through the preceding CME and not due to the CME–CME interaction. The results also highlight the importance of the comparison of solar wind proton velocity data with the expected temperature data, in particular, to understand the ICME–ICME interaction processes.

1 Introduction

Coronal mass ejections (CMEs) are large expulsions of plasma and magnetic field from the Sun, which have propagation speeds ranging from a few hundred to a few thousand kilometers per second. Depending upon their initial speeds, their travel time from the Sun to the Earth is known to range from 1 to 4 days. Around solar maximum, the number of CMEs launched from the Sun is approximately five per day ([St. Cyr et al., 2000](#); [Yashiro et al., 2004](#); [Webb and Howard, 2012](#)) in contrast to one CME in 5 days during the solar minimum phase ([St. Cyr et al., 2000](#); [Gopalswamy et al., 2005](#); [Gopalswamy et al., 2006](#); [Webb and Howard, 2012](#)). It is also well known that, generally, homologous CMEs originate from the same active region and exhibit a close morphological resemblance in coronal

Abstract

1 Introduction

2 Observations

3 Data analysis

4 Results and discussion

5 Conclusion

Data availability statement

Author contributions

Funding

Acknowledgments

Conflict of interest

Publisher's note

References

 Export citation ▾


Check for updates

We use cookies

Our website uses cookies that are essential for its operation and additional cookies to track performance, or to improve and personalize our services. To manage your cookie preferences, please click Cookie Settings. For more information on how we use cookies, please see our [Cookie Policy](#).



Articles

Research Topics

Editorial board

effectiveness due to the extended period and enhanced strength of the southward magnetic field, which are responsible for causing intense geomagnetic storms ([Wang et al., 2003](#); [Farrugia and Berdichevsky, 2004](#); [Farrugia et al., 2006](#); [Lugaz et al., 2013](#); [Lugaz et al., 2017](#)).

As the CMEs interact in the heliosphere, it is expected that the participating CME will either merge to form a single interplanetary CME with different properties than those of the participating CMEs or will arrive as distinct entities of ICMEs at 1 AU, retaining their original properties. Merging of CMEs is expected when reconnection can set in between the trailing edge of the preceding CME and the leading edge of the following CME, resulting in a single flux rope ([Palmerio et al., 2021](#)). Simulation studies on the resulting magnetic structure of interacting CMEs carried out by [Schmidt and Cargill \(2004\)](#) and [Lugaz et al. \(2013\)](#) show that, in general, two flux ropes with the opposite orientation offer favorable configuration for efficient magnetic reconnection during the interaction, in particular at the interface between the two flux ropes, where antiparallel fields meet. [Kilpua et al. \(2019\)](#) provided supporting observations for the aforementioned simulation results for the interacting CMEs of June 2012, investigated in the present study. However, irrespective of the orientation of the flux rope between the interacting ICMEs, there is always a radial compression of the preceding CME as the shock driven by CME2 propagates through CME1. When the axial fields of the two CMEs are antiparallel, there is often a short period of overexpansion following the interaction as the rate of overexpansion depends partly on the reconnection rate between the two CMEs

Articles

published
with
Frontiers
have
received
12 million
total
citations

Your
research is
the real
superpower
- learn how
we
maximise
its impact
through
our leading
community
journals

[Explore our impa](#)

People also
looked at

Global insight
into a complex-
structured
heliosphere

We use cookies

Our website uses cookies that are essential for its operation and additional cookies to track performance, or to improve and personalize our services. To manage your cookie preferences, please click Cookie Settings. For more information on how we use cookies, please see our [Cookie Policy](#).

In addition to plasma and magnetic parameters, the other class of signatures, which is important, are the composition signatures of the ICMEs ([Zurbuchen and Richardson, 2006](#)). Therefore, it is crucial to examine and understand the observations of composition parameters in interacting ICMEs. In the present study, we aim to understand the space weather effects of the interacting CMEs in the heliosphere in the context of composition signatures.

The charge state distributions of heavy ions in ICMEs observed in the *in situ* data generally provide information on the conditions prevalent in the corona where the CME plasma originates. The charge state has been used to distinguish fast wind from slow wind ([von Steiger and Zurbuchen, 2003](#)) as they originate from different source regions in the corona, i.e., coronal holes and streamers, respectively. It is also to be noted that the timescale needed for solar wind expansion is typically much shorter than that of ionization and recombination, thereby freezing-in the relative ionization states and maintaining the values that are present at the source region ([Hundhausen et al., 1968](#)). This suggests that the ionic fractions measured *in situ* are dictated by the physical parameters near the Sun where freeze-in occurs ([Rakowski et al., 2007; Gruesbeck et al., 2011; Gruesbeck et al., 2012; Lynch et al., 2011; Song et al., 2015a; Song et al., 2015b](#)), which have been further used to infer the eruption process of flux ropes ([Song et al., 2016; Wang et al., 2017; Huang et al., 2018](#)). The high ionization states refer to a hot source region and can also describe the thermal history of the interplanetary plasmas by comparing the freezing-in temperatures of

Radial Sizes and Expansion Behavior of ICMEs in Solar Cycles 23 and 24

Wageesh Mishra,
Urmi Doshi and
Nandita Srivastava

A prominence eruption from the Sun to the Parker Solar Probe with multi-spacecraft observations

Tatiana Niembro,
Daniel B. Seaton,
Phillip Hess, David Berghmans,
Vincenzo Andretta,
Katharine K. Reeves,
Pete Riley, Michael L. Stevens, Federico Landini, Clementina Sasso, Cis Verbeeck, Roberto Susino and Michela Uselenghi

We use cookies

Our website uses cookies that are essential for its operation and additional cookies to track performance, or to improve and personalize our services. To manage your cookie preferences, please click Cookie Settings. For more information on how we use cookies, please see our [Cookie Policy](#).

CMEs may give rise to a higher fraction of ionization in the following CME plasma.

and Harry P. Warren

Furthermore, CME–CME interactions can lead to different compositional signatures through the mixing of plasma from the two CMEs. This suggests the possibility that plasma from one CME can become entrained within the other CME, which can further lead to a sequence of multiple or longer duration peaks of compositional signatures than those in an isolated ICME.

Coalescence of Magnetic Flux Ropes Within Interplanetary Coronal Mass Ejections: Multi-cases Studies

Yan Zhao,
Hengqiang Feng,
Qiang Liu and
Guoqing Zhao

In the case of isolated CMEs, the well-known composition signatures are the enhanced alpha to proton ratio, and elevated Fe/O , C^{+6}/C^{+5} , and O^{+7}/O^{+6} ratios (Henke et al., 2001; Lepri et al., 2001; Zurbuchen et al., 2003; Kilpua et al., 2017). Furthermore, in interacting CMEs, it is expected that the charge state of elements will show enhancement with several peaks in between. These peaks may be associated with the arrival of distinct CMEs or different solar wind structures arising due to participating CMEs in the interaction. The interacted CME structures are generally marked by signatures of complex ejecta (Burlaga et al., 2002), which are enhanced for a duration of more than 2 days (Rodkin et al., 2018), implying that composition signatures of interacting CMEs can last longer than those of isolated CMEs (Temmer et al., 2017). Furthermore, the ion composition of ICMEs are generally associated with the solar source regions of CMEs and are frozen-in; therefore, they are expected to remain unaltered during their heliospheric propagation. The ion charge state and mass composition of solar wind plasma can, therefore, be used to identify various components of ICMEs and their source regions (Fisk et al., 1998; Zhao et al., 2009; 2014; Kilpua et al., 2014;

We use cookies

Our website uses cookies that are essential for its operation and additional cookies to track performance, or to improve and personalize our services. To manage your cookie preferences, please click Cookie Settings. For more information on how we use cookies, please see our [Cookie Policy](#).

composition of CME plasma and its evolution largely depend upon the temperature, density, mass, and velocity. The typical composition parameters of ICMEs, as reported by Zurbuchen and Richardson (2006) and Rodkin et al. (2017), are as follows: proton speed $\sim 450 \text{ km}\cdot\text{s}^{-1}$, proton temperature as $< 5 \times 10^5 \text{ K}$, $\text{Na}/\text{Np} > 8\%$, $\text{C}^{+6}/\text{C}^{+5} > 1$, $\text{O}^{+7}/\text{O}^{+6} > 0.8$, $\text{Fe}/\text{O} > 0.2$, $Q_{\text{Fe}} > 12$, and B is 3–40 nT (Table 1). In contrast, the respective composition parameters of the normal solar wind are $360 \text{ km}\cdot\text{s}^{-1}$, $6 \times 10^4 \text{ K}$, $\text{Na}/\text{Np} < 8\%$, $\text{C}^{+6}/\text{C}^{+5} < 1$, $\text{O}^{+7}/\text{O}^{+6} < 0.8$ $\text{Fe}/\text{O} \approx 0.1$, Q_{Fe} is 9–11, and B is 4 nT (Table 1). Furthermore, Gopalswamy et al. (2013) found that faster CMEs have higher ion charge states than the slower CMEs. In another study, the typical parameters of ion charge states, as reported for ICMEs in the ascending phase of the solar cycle, are marked by Q_{Fe} ranging from 10.2 to 17.6 (max) and the average value is 10.8. The $\text{O}^{+7}/\text{O}^{+6}$ ratio reported for the same period has an average of 0.34 and the maximum value ranges from 0.2 to 1.5 (Rodkin et al., 2017).

Table 1

	Average V ₀ (km/m)	T _p (C)	Peak %	C ₁₀ ² /C ₁₀ ⁴	D ₁₀ ² /D ₁₀ ⁴	Fe/ ₂ O ₃	Q ₉₀	Average Initial E (T)	
Solar wind	300			$\approx 10^2$	~4%	<1	~0.5	~0.5	~1.1
Typical WCR	450			$\approx 10^2$	~1%	<1	~0.5	~0.2	~3-40
Hot events	450			$\approx 10^2$	~2%	<1	~0.5	~0.5	~10

TABLE 1.
Composition
signatures of
normal solar wind,
isolated ICMEs,
and the June and
November 2012

We use cookies

Our website uses cookies that are essential for its operation and additional cookies to track performance, or to improve and personalize our services. To manage your cookie preferences, please click Cookie Settings. For more information on how we use cookies, please see our [Cookie Policy](#).



Articles

Research Topics

Editorial board

magnetic field component along with elevated values of the dynamic pressure. This can further result in intense geomagnetic storms and also trigger substorms. Therefore, it is of interest to investigate whether observations suggest that the interaction of CMEs leads to compression. A previous study by [Elliott et al. \(2005\)](#) on compression and rarefaction of solar wind/CME structures suggested that any compression leads to heating of the plasma. This occurs as the fast solar wind stream overtakes the slow solar wind stream and is accompanied by an increase in the solar wind speed. In rarefaction, cooling occurs and proton speed decreases when the fast solar wind stream surpasses the slow solar wind stream. [Elliott et al. \(2005\)](#) fit the proton temperature and velocity ($T_p - V$) curves separately for compression and rarefaction and found that the expected temperature is given by $T_{\text{exp}} = 640V - 1.56 \times 10^5$ (for compression) and $T_{\text{exp}} = 459V - 1.18 \times 10^5$ (for rarefaction).

In this paper, we examine the time profiles of the ion charge composition of two interacting CME events observed in the year 2012. We attempt to identify the sources of the ICMEs and the corresponding composition signatures at L1, with structures corresponding to their sources on the solar surface. We also examine the signatures of compression and rarefaction of ICMEs estimated from the expected temperature and compare them with the proton velocity observations recorded by *in situ* instruments.

2 Observations

In the present study, we have analyzed the composition parameters of two events of the

We use cookies

Our website uses cookies that are essential for its operation and additional cookies to track performance, or to improve and personalize our services. To manage your cookie preferences, please click Cookie Settings. For more information on how we use cookies, please see our [Cookie Policy](#).

data and hourly averaged latitude (δ) and longitude (ϕ) values of the interplanetary magnetic field from the OMNI database (<https://cdaweb.gsfc.nasa.gov>).

We mark the time of arrival of shock and the start and end time of the ICMEs based on the Richardson–Cane (RC) catalog ([Richardson and Cane, 2004](#); [Richardson and Cane, 2010](#)) for the two events. It is important to mention that in the RC catalog (<https://izw1.caltech.edu/ACE/ASC/DATA/level3/icmetable2.htm>), the ICME timings are based primarily on plasma and magnetic field signatures ([Cane and Richardson, 2003](#)).

3 Data analysis

As mentioned in the previous section, for the present study, we selected two cases of interacting CMEs, which showed distinct signatures in *in situ* observations of plasma and magnetic parameters at L1, as identified from the RC catalog. The first CME–CME interaction event was observed during 13–14 June 2012 which resulted in a merged structure and has been reported in detail by [Srivastava et al. \(2018\)](#). The second event of 9–10 November 2012 resulted in two distinct structures separated by an interaction region and has been discussed in depth by [Mishra et al. \(2015a\)](#). In what follows, we discuss the composition parameters and their evolution with time for the two events separately.

3.1 Interacting CMEs of 13–14 June 2012

As reported by [Srivastava et al. \(2018\)](#), two CMEs were launched from the same active region NOAA

We use cookies

Our website uses cookies that are essential for its operation and additional cookies to track performance, or to improve and personalize our services. To manage your cookie preferences, please click Cookie Settings. For more information on how we use cookies, please see our [Cookie Policy](#).

ICMEs, it was found that it led to the strongest sudden storm commencement (SSC) (~ 150 nT) of the solar cycle. The SSC was unique because of its long duration of approximately 20 h. **Figure 1A** shows the plasma and magnetic properties of the interacting CMEs of June 13 and 14, as observed at L1 during 17–18 June 2012. The times of the observed CMEs of 13 and 14 June 2012 and the associated flares are tabulated in **Table 2**.

Figure 1

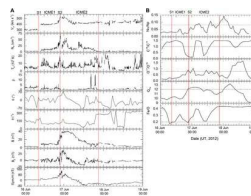


FIGURE 1. (A) Plasma and magnetic parameters observed in situ by the ACE spacecraft for the interacting CMEs of 13–14 June 2012. From the left, the first, second, and third vertical red lines mark the arrival of shock (S1) associated with CME1, shock (S2) associated with CME2, and the trailing boundary of ICME2, respectively. (B) Composition

We use cookies

Our website uses cookies that are essential for its operation and additional cookies to track performance, or to improve and personalize our services. To manage your cookie preferences, please click Cookie Settings. For more information on how we use cookies, please see our [Cookie Policy](#).

mark the arrival of shock (S1) associated with CME1, shock (S2) associated with CME2, and the trailing boundary of ICME2, respectively, as identified by plasma signatures in (A). The threshold values for the compositional signatures are marked as horizontal dash lines.

Table 2

Start Date	CME Date	Reversal Duration (DT)	Peak Lat.	CME-Associated EIT	Off-Associated EIT
2012-06-13T00:00:00Z	2012-06-13T00:00:00Z	~10 min	~50°	Present	N/A
2012-06-14T00:00:00Z	2012-06-14T00:00:00Z	~10 min	~50°	Present	N/A

TABLE 2. CME and associated flare characteristics for the 13–14 June 2012 event.

We plotted the plasma and magnetic parameters of the interacting ICMEs of June as observed by

We use cookies

Our website uses cookies that are essential for its operation and additional cookies to track performance, or to improve and personalize our services. To manage your cookie preferences, please click Cookie Settings. For more information on how we use cookies, please see our [Cookie Policy](#).

(ICME) of approximately 14 hr duration during 22.12 UT on June 16–12:31 UT on June 17. During this period, the plasma β value remained less than 1, the total magnetic field B remained higher than 10 nT, and the magnetic field angle θ rotated from +70° to -70°, fulfilling the criteria of a MC as defined by [Burlaga et al. \(1981\)](#).

3.1.1 Composition signatures

The ICMEs and associated shocks observed at the L1 point by the ACE and WIND spacecraft, corresponding to the June event, are tabulated in [Table 3](#). Among other parameters, the profiles of composition parameters like average values of Q_{Fe} and the O^{+7}/O^{+6} ratio during the passage of ICMEs, as measured at L1, were plotted. The O^{+7}/O^{+6} parameter is temperature dependent, and the Fe/O parameter is known to be magnetic structure dependent ([Rodkin et al., 2018](#)). Since the solar wind ion charge states “freeze-in” within a few solar radii from the Sun, ICMEs show an increased abundance of high-charge states. For example, the O^{+7}/O^{+6} ratio is greater than 1.0 in the majority of the ICMEs ([Henke et al., 2001](#)), and it serves as a good signature of the hot plasma (increased electron temperature) in the structure of MCs. On the other hand, the elemental ratios depend on chromospheric temperatures, the magnetic field configuration at the origin of the plasma, and the plasma confinement time before the release [e.g., [Laming \(2015\)](#), and references therein]. In ICMEs, increased amounts of high-charge states of elements, such as Fe, Ne, Si, and Mg, are often observed, suggesting extended confinement times [e.g., [Lepri et al. \(2001\)](#); [Zurbuchen et al. \(2016\)](#)]. We note the maximum values of the aforementioned parameters and also the average values during the passage of

We use cookies

Our website uses cookies that are essential for its operation and additional cookies to track performance, or to improve and personalize our services. To manage your cookie preferences, please click Cookie Settings. For more information on how we use cookies, please see our [Cookie Policy](#).

ICME	ICME date	ICME start date	ICME end date	ICME duration	ICME end date	ICME duration
1	2012-06-13	2012-06-13	2012-06-14	2012-06-14 - 2012-06-13	2012-06-14	2012-06-14 - 2012-06-13
2	2012-06-13	2012-06-13	2012-06-14	2012-06-14 - 2012-06-13	2012-06-14	2012-06-14 - 2012-06-13

TABLE 3. IP shocks and ICMEs associated with the 13–14 June 2012 CMEs.

In the case of the interacting CMEs of June 2012, on the basis of the composition parameters, we note that ICME1 has $Na/Np > 0.6$, $C^{+6}/C^{+5} > 1.5$, and $O^{+7}/O^{+6} > 0.6$ (only in the trailing edge). The Fe/O ratio is > 0.2 in the middle of ICME1; $Q_{Fe} > 12$ in the trailing edge and the average value of B lies in the range of 1–10 nT. This seems to be a relatively smaller enhancement than the background solar wind. However, close to the trailing end of the ICME (boundary identified using the plasma parameters), the value of B is enhanced to 10–20 nT in ICME1.

ICME1 is followed by the passage of the second shock and then an MC, wherein the O^{+7}/O^{+6} values varied between 1.0 and 0.2, Fe/O varied from 0.2 to 0.4, and Q_{Fe} from 12 to 10. C^{+6}/C^{+5} increased from 0 to 1.5 and finally decreased to 0. The Na/Np ratio showed a gradual increase from the leading to the trailing edge of the MC and also marked the enhancement with two peaks. These values of compositional parameters are in good agreement with those reported for fast MCs ([Gopalswamy et al., 2013](#)). Such fast MCs (mean $934 \text{ km}\cdot\text{s}^{-1}$) have been reported with the O^{+7}/O^{+6} value exceeding 0.6 and $Q_{Fe} > 11$ ([Table 4](#)).

We use cookies

Our website uses cookies that are essential for its operation and additional cookies to track performance, or to improve and personalize our services. To manage your cookie preferences, please click Cookie Settings. For more information on how we use cookies, please see our [Cookie Policy](#).

As mentioned in Sections 3.1, conventionally, the ICME boundaries are defined based on the plasma and magnetic signatures of ICMEs ([Cane and Richardson, 2003](#)). However, some authors also take composition signatures into consideration to mark the ICME boundaries ([Lepping et al., 1997](#); [Lepri et al., 2001](#); [Huttunen et al., 2005](#); [Richardson and Cane, 2010](#)).

We have compared the ICME boundaries of these interacting CMEs derived from plasma and magnetic parameters with those derived from the composition parameters. For this purpose, we identify the boundaries within which Q_{Fe} and the O^{+7}/O^{+6} ratio remain above the threshold values. Normally, these values are expected to drop to their normal or threshold values after the passage of the ICMEs. However, in a few cases, the composition parameters do not show the expected decrease. As per the aforementioned criteria, we marked the end of the ICME boundary at 14:00 h on June 18, which suggests that the duration of the ICME is extended by approximately 17 h compared to that defined by the plasma parameters.

The ICME duration as obtained from the plasma and magnetic field parameters, i.e., from June 16, 9:00 UT to June 17, 21:00 UT, is approximately 36 h, which is close to the mean values of a normal ICME duration ([Dasso et al., 2009](#); [Lugaz et al., 2013](#); [Lugaz and Farrugia, 2014](#); [Lugaz et al., 2015](#)). However, if we include the charge state signatures, the duration of the June event is estimated to be approximately 53 h. This increased duration in charge state enhancement has also been reported previously for isolated ICMEs ([Lepri et al., 2001](#); [Richardson and Cane,](#)

We use cookies

Our website uses cookies that are essential for its operation and additional cookies to track performance, or to improve and personalize our services. To manage your cookie preferences, please click Cookie Settings. For more information on how we use cookies, please see our [Cookie Policy](#).

distributed hot plasma components but correspond to the inhomogeneous plasma and magnetic structure of the participating CMEs.

3.1.3 Associated flares and ICME composition

The associated flares with the interacting CMEs in the June event are M-class flares, i.e., M1.2 and M1.9 class, respectively. As mentioned previously, the two flares originated in the same active region NOAA AR 11504, located at around S16E18 on 13 June 2012. It is expected that heating during the early rise phase of CMEs will create very high ionic charge states. The charge state values reached may depend on the amount of energy available through reconnection and related processes and also on the amount of energy available for the associated flare. Furthermore, the heating and associated acceleration of the CME can drag the heavier elements from the lower corona and carry further out. It was suggested that the physical mechanisms causing heavier elements in the ICME flux ropes and those leading to higher ionization states of elements in ICMEs are related (Reinard, 2008), although it may have some spatial dependence, i.e., different plasma parcels may get affected differently by these mechanisms during the eruption. Reinard (2005) reported that all CMEs show a slight-to-moderate correlation between the charge states and the associated flare magnitude or class. They noticed that O^{+7}/O^{+6} and Q_{Fe} are better correlated when the *in situ* spacecraft is likely to cross the center of the CME ejecta (i.e., between E30 and W45). Furthermore, they conclude that the charge states in these “central events” display a moderate correlation with flare magnitude, indicating that enhanced charge states in the solar wind are the result of flare-related heating in the corona. For June 2012

We use cookies

Our website uses cookies that are essential for its operation and additional cookies to track performance, or to improve and personalize our services. To manage your cookie preferences, please click Cookie Settings. For more information on how we use cookies, please see our [Cookie Policy](#).

SECTION I, we calculated the expected proton temperature values for compression and rarefaction for preceding and following ICMEs separately for the June event. The empirical formulae by Elliott et al. (2005) are based on ACE data for the estimation of the expected solar wind proton temperature. These formulae should hold good for data obtained by any spacecraft located at the L1 point. Furthermore, it is to be noted that minor variations are expected in the formulae derived from observations by different spacecraft located close to L1, e.g., WIND, ACE, STA, and STB, primarily due to the different heliocentric distances of the probes (Yu et al., 2016). However, as the empirical relationship is derived from a statistical study over a certain period of the solar cycle, we expect the overall trend (within error bars) to remain the same for the selected ICMEs in our study. Figure 2 shows the variation of the observed proton velocity V_p (lower panel), proton temperature T_p (black curve), and overplotted expected temperatures for compression and rarefaction (red and blue curves) in the upper panel.

Figure 2

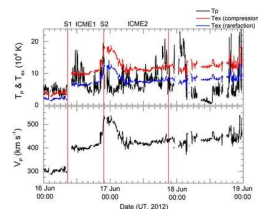


FIGURE 2.

Variation of the proton velocity, proton temperature, and overplotted expected

We use cookies

Our website uses cookies that are essential for its operation and additional cookies to track performance, or to improve and personalize our services. To manage your cookie preferences, please click Cookie Settings. For more information on how we use cookies, please see our [Cookie Policy](#).

for the same events in [Figure 2](#), we examine whether the majority of the data points lie close to the compression or rarefaction profiles. Furthermore, we corroborate the same by comparing with the observed proton velocity data (lower panel). From [Figure 2](#), we note that the expected temperature for ICME1 at the leading and trailing edge shows compression, while the central part shows rarefaction. However, the observed proton velocity is clearly close to compression during ICME1 and does not show any signatures of rarefaction at the central part. Based on the expected temperature profile for ICME2, the leading edge, trailing edge, and central part all show rarefaction. However, the observed proton velocity plot shows signatures of rarefaction in the leading edge only, and compression in the central and trailing part of ICME2.

This analysis clearly suggests the importance of comparing the expected temperature profile with that of the observed proton temperature and speed profile, particularly in the case of the CME–CME interaction.

3.2 Interacting CMEs of 9–10 November 2012

Another interaction event was recorded in the same phase of solar cycle 24 when two CMEs with similar 3D speeds $620 \text{ km}\cdot\text{s}^{-1}$ and $910 \text{ km}\cdot\text{s}^{-1}$ were launched within a 24-h period on 9 and 10 November 2012 from NOAA AR 11608. These CMEs propagated in the same direction and were observed to interact at a distance of $35 R_{\odot}$ from the Sun. The detailed study of this interaction event by [Mishra et al. \(2015a\)](#) showed that it led to

We use cookies

Our website uses cookies that are essential for its operation and additional cookies to track performance, or to improve and personalize our services. To manage your cookie preferences, please click Cookie Settings. For more information on how we use cookies, please see our [Cookie Policy](#).

Event	CME Date	Associated ICME date (UT)	Periodicity	ICME duration (UT)	ICME speed (km/s)
1	2012-Nov-09	2012-Nov-10	40.0	2012-Nov-10	400
2	2012-Nov-09	2012-Nov-10	10.0	2012-Nov-10	400

TABLE 5. CME and associated flare characteristics for the 9–10 November 2012 event.

Table 6

Event	ICME date	Start date	CME start date	CME end date	ICME start date	ICME end date	ICME speed (km/s)
1	2012-Nov-10	2012-Nov-10	2012-Nov-10	2012-Nov-10	2012-Nov-10	2012-Nov-10	400
2	2012-Nov-10	2012-Nov-10	2012-Nov-10	2012-Nov-10	2012-Nov-10	2012-Nov-10	400

TABLE 6. IP shocks and ICMEs associated with the 9–10 November 2012 CMEs.

3.2.1 Composition signatures

From [Figure 3](#), we note that the first ICME is an MC based on the criteria of [Burlaga et al. \(1981\)](#). Prior to the arrival of ICME, a long-duration sheath region was observed from 12 November 22:20 UT to 13 November 08:52 UT. An enhancement of the alpha to proton ratio was observed from ~ 2% to 10% in the sheath region. The value of C^{+6}/C^{+5} dropped from ~ 1 to 0.3, O^{+7}/O^{+6} ratio from ~ 0.1 to 0.7, Q_{Fe} increased from ~ 10.5 to 12.8, and Fe/O ranged between ~ 0.3 and 0.4 in the sheath region.

We use cookies

Our website uses cookies that are essential for its operation and additional cookies to track performance, or to improve and personalize our services. To manage your cookie preferences, please click [Cookie Settings](#). For more information on how we use cookies, please see our [Cookie Policy](#).



Articles

Research Topics

Editorial board

CMEs of 9–10

November 2012.
The vertical lines
marked in red,
from left to right,
denote the arrival
of the shock,
ICME1 leading and
trailing boundaries,
ICME2 leading and
trailing boundaries.
Between the third
and fourth vertical
lines are marked
by a small
interaction region
(IR) in between the
two ICMEs. (B)
Composition
parameters
marking the arrival
of ICMEs
associated with
the interacting
CMEs of
November 2012.
Here, again the
vertical lines
marked in red
denote, from left
to right, the arrival
of shock, ICME1
leading and trailing
boundaries, ICME2
leading and trailing
boundaries, as
identified by
plasma signatures

We use cookies

Our website uses cookies that are essential for its operation and additional cookies to track performance, or to improve and personalize our services. To manage your cookie preferences, please click Cookie Settings. For more information on how we use cookies, please see our [Cookie Policy](#).

The sheath region was followed by a long-duration MC from 13 November 08:52 UT to 14 November 02:25 UT. In the MC region, the O^{+7}/O^{+6} ratio ranged between ~ 0.4 and 0.9 , which is enhanced compared to a normal ICME (>0.6). Values of the Fe/O ratio ranged between ~ 0.2 and 0.4 , Q_{Fe} ranged between ~ 10.5 and 13 , C^{+6}/O^{+5} from ~ 0.3 to 1.5 , and the alpha to proton ratio increased from $\sim 4\%$ to 10% (Table 7). All the composition signatures showed similar enhancement as in the case of the June 2012 event and are in agreement with those reported for MCs previously (Gopalswamy et al., 2013). After the passage of the MC, a small interaction region was observed between 14 November 02:25 UT and 12:00 UT. This region was marked by a decrease in the constant values of $C^{+6}/O^{+5} \sim 0.6$ and O^{+7}/O^{+6} as ~ 0.05 , and the almost constant value of $Q_{Fe} \sim 9.5 - 10$ and $Fe/O \sim 0.3 - 0.4$.

Table 7

Start of CME	End of CME	ICME boundary date/time	ICME boundary date/time	N_2^{+}	C^{+6}	O^{+7}	O^{+6}	Fe/O	Q_{Fe}	C^{+6}/O^{+5}	O^{+7}/O^{+6}
Nov 13 08:52	Nov 14 02:25	Nov 13 08:52	Nov 14 02:25	~0.05	~0.3	~0.4	~0.6	~0.3	~10.5	~0.6	~0.05

TABLE 7.
Compositional
parameters of
November 2012
ICMEs.

We use cookies

Our website uses cookies that are essential for its operation and additional cookies to track performance, or to improve and personalize our services. To manage your cookie preferences, please click Cookie Settings. For more information on how we use cookies, please see our [Cookie Policy](#).



magnetic field topology in the source region at the Sun, the behavior of the Fe/O parameter in this case suggests that the interacting CME events comprise plasma of different magnetic structures. It is interesting to note that other important composition parameters like the enhanced values of the O^{+7}/O^{+6} ratio and $Q_{Fe} > 12$ do not extend to the interaction region and ICME2. This is suggestive of the fact that although different magnetic structures are present in the ICME, the temperature is not high enough, as for typical ICMEs ([Table 1](#)).

On the basis of the composition parameters, we found that the ICME duration is extended by 15 h, i.e., up to 22:00 UT 14 November 2012. The identified ICME boundaries are in accordance with those reported by [Mishra et al. \(2015a\)](#). It is important to mention that the total duration of the ICME is ~46 h if the composition signatures are considered.

Furthermore, as observed for the June event, in this case also, out of the total ICME duration, the charge state enhancement is observed only for a short period and not continuously throughout the ICME. The times for enhancement of the different parameters Na/Np , Q_{Fe} , O^{+7}/O^{+6} , C^{+6}/C^{+5} , and Fe/O are reported for ~34%, ~26%, ~22%, ~32%, and ~30% of the total duration of the ICME in the present case, respectively. This result reconfirms that interacting CMEs do not comprise uniformly distributed hot plasma components, as was found for the June event.

3.2.3 Associated flares and ICME composition

The associated flares with the interacting CMEs in the November event are of the B5.2 and C2.0 flare

We use cookies

Our website uses cookies that are essential for its operation and additional cookies to track performance, or to improve and personalize our services. To manage your cookie preferences, please click Cookie Settings. For more information on how we use cookies, please see our [Cookie Policy](#).

the maximum values of the aforementioned parameters are ~ 0.86 , ~ 12.42 , and ~ 0.09 , respectively, which are indicative of the presence of ICME hot plasma.

The stronger a flare is, the hotter the flare plasma is expected to be, which is directly related to the enhancements in the ionic composition signatures of the ICMEs. To the best of our knowledge, no study showing that flare intensity dictates the duration of the compositional signatures has been reported previously. However, we expect that the duration of the compositional signatures will strongly depend on the relative position of the intercepting *in situ* spacecraft with respect to the central core of the ICME/flux rope. This is because the enhanced ionic and elemental composition associated with the CME flux rope system can drag additional material along with it, including the overlying plasma that are magnetically connected, creating an envelope of material that indirectly and only partially participates in the eruption. Therefore, an *in situ* spacecraft intercepting the central part of the flux rope system can observe enhanced elemental and ionic compositional signatures of ICMEs.

3.2.4 Relationship between the expected and observed proton temperatures with proton velocity

Similar to the June event, we calculated the expected temperature T_{exp} for compression and rarefaction for preceding and following ICMEs of the November event ([Figure 4](#)). We note that during ICME1, the expected temperature at the leading edge suggests compression, although the central part and trailing edge clearly suggest rarefaction. On the contrary, the observed proton

We use cookies

Our website uses cookies that are essential for its operation and additional cookies to track performance, or to improve and personalize our services. To manage your cookie preferences, please click Cookie Settings. For more information on how we use cookies, please see our [Cookie Policy](#).

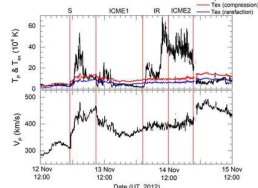
Figure 4.

FIGURE 4.
Variation of the proton velocity, proton temperature, and overplotted expected temperature of compression and rarefaction for interacting CMEs of the 9–10 November 2012 event.

4 Results and discussion

The two interacting CME events of June and November 2012 occurred in the rising phase of solar cycle 24. These two events manifested different structures at 1 AU in *in situ* data after the interaction of the associated CMEs. The composition and compression signatures of the two interacting events were examined.

4.1 Composition signatures of the interacting events

Our analysis shows that the boundaries for the two interacting ICME events defined by plasma and magnetic parameters differ from those defined by composition parameters. The durations of the two events of interacting CMEs are 53 h (2.2 days) and 48 h (2.0) respectively as found on

We use cookies

Our website uses cookies that are essential for its operation and additional cookies to track performance, or to improve and personalize our services. To manage your cookie preferences, please click Cookie Settings. For more information on how we use cookies, please see our [Cookie Policy](#).

the association of different classes of flares in the two events. In the June 2012 case, both the flares were M-class flares, wherein the charge state enhancement was observed. In the second case of the November 2012 events, the charge state enhancement is not significant as the associated flares are only B- and C-class flares. Accordingly, the Fe charge state enhancement is less in the November event than that in the June events. This is further attributed to the fact that the Fe charge state is strongly related to flare class and temperature (Reinard, 2008).

The analysis also reveals that the duration of the charge state enhancement above the threshold values is considerably smaller than the total ICME duration derived from the solar wind plasma and magnetic parameters and ranges between ~30% and 35%, suggesting that the charge state enhancement is not uniform throughout the complex structures of the interacting CMEs that arrive at the Earth.

The maximum and average values of Q_{Fe} and O^{+7}/O^{+6} for the two interacting CME events are representative of the values for isolated ICMEs observed in SC24 and are lower than those observed in SC23 (Gopalswamy et al., 2013). Furthermore, the interacting CMEs are released from the Sun in succession at an interval of 24 h, and usually, the interaction of two distinct CMEs is expected to occur farther out in the corona, where the chances of the two CME plasmas mixing are remote and one would, therefore, presume that the two participating CMEs would retain the composition signatures of the associated flares. This is why charge state values of the corresponding CMEs are in agreement with

We use cookies

Our website uses cookies that are essential for its operation and additional cookies to track performance, or to improve and personalize our services. To manage your cookie preferences, please click Cookie Settings. For more information on how we use cookies, please see our [Cookie Policy](#).

June events: As discussed in the previous section, based on the expected temperature data, we find that ICME1 leading and trailing edges show signatures of compression in the June event. However, the central part of ICME1 appears to be rarefied as the observed temperature is lower than the expected temperature. We further note that the duration of ICME1 is approximately 12 h, out of which for approximately 8 h, the ICME is compressed. For 4 h only, we observe signatures of rarefaction in the temperature data. For the entire ICME1, the observed constant value of the proton velocity data reveals that the CME is significantly compressed.

As it is difficult to identify the signatures of compression or rarefaction in the mid region of ICME1 based on the proton velocity data alone, this essentially highlights the importance of the comparison of solar wind proton velocity data with the expected temperature data, in particular to understand the ICME–ICME interaction processes.

Furthermore, the expected proton temperature profile reveals that ICME2 underwent rarefaction. However, the observed proton velocity plot shows rarefaction in the leading part, and the trailing part is moderately compressed as it remains constant.

November events: In this particular case, the expected proton temperature profile suggests moderate compression in the leading part of ICME1. On the other hand, the trailing part of ICME1 showed clear signatures of over-rarefaction. The proton velocity signified rarefaction during the leading part, as is also evident by a decrease of proton speed, suggesting

We use cookies

Our website uses cookies that are essential for its operation and additional cookies to track performance, or to improve and personalize our services. To manage your cookie preferences, please click Cookie Settings. For more information on how we use cookies, please see our [Cookie Policy](#).



expected temperature and proton velocity data.

Such signatures of heating may be attributed to a probable flank encounter of the following ICME2 with the *in situ* spacecraft, as also reported by [Mishra et al. \(2015a\)](#) for the same event.

A comparison of June and November interacting CME events shows that ICME1 shows a signature of compression and ICME2 shows clear rarefaction in the June event. However, in the November case, ICME1 shows a signature of rarefaction, but during the interacting region and ICME2, clear signatures of compression are noted. The analysis of observations also suggests that if the following CME is not driving a strong shock, it is unlikely that the preceding CME will get compressed. Basically, our study supports the idea that compression can occur due to the passage of the shock associated with the following CME through the preceding CME and not the CME–CME interaction.

5 Conclusion

Among other parameters of solar transients or ICMEs, the ion charge composition of the plasma is one of the crucial identifiers of their source regions for isolated CMEs. In this study, we investigate the ion charge state evolution of the ICME plasma by considering the ratios of alpha to proton, carbon, C^{+6}/O^{+5} , and oxygen, O^{+7}/O^{+6} , Fe/O , and the average charge of iron ions, Q_{Fe} , which were measured *in situ* with ACE. Although the ion charge states of interacting CMEs are not expected to be altered by the interaction process, the ion composition profiles in interacting events, at 1 AU, are difficult to interpret and depend on the parameters of the participating CMEs, their

We use cookies

Our website uses cookies that are essential for its operation and additional cookies to track performance, or to improve and personalize our services. To manage your cookie preferences, please click Cookie Settings. For more information on how we use cookies, please see our [Cookie Policy](#).

1. The two reported events of 12–13 June 2012 and 9–10 November 2012, were accompanied by M-class flares or below. The associated CMEs also had moderately high speeds ranging from 560 to 900 km·s⁻¹. Both CMEs were associated with MCs that displayed strong composition signatures.
2. In the CME–CME interaction events, the ion composition profiles can have several peaks corresponding to the plasma temperatures in the individual solar sources/flares of associated ICMEs. In the interacting CMEs reported here, the ion composition profiles displayed several maxima, suggesting the inhomogenous nature of plasma due to the participating CMEs. As in this case, CME plasma mixing is generally not expected and the peak values of O⁺⁷/O⁺⁶ and Q_{Fe} correspond to the plasma temperatures in the individual solar sources of these CMEs.
3. The duration of interacting CMEs is found to be twice as long, as found for the individual CMEs, if the boundaries are identified, based on the composition parameters.
4. It is also concluded that the duration of the charge state-enhanced plasma in the interacting CME events is shorter and that they are observed for approximately 35% or less of the entire duration of the ICME, implying the passage of different magnetic structures with plasma at different temperatures.
5. The study reconfirms the finding of previous studies ([Lugaz et al., 2005](#); [Liu et al., 2012](#); [Mishra et al., 2015b](#); [Lugaz et al., 2016](#); [Srivastava et al., 2018](#)), which showed that compression can occur due to the passage of

We use cookies

Our website uses cookies that are essential for its operation and additional cookies to track performance, or to improve and personalize our services. To manage your cookie preferences, please click Cookie Settings. For more information on how we use cookies, please see our [Cookie Policy](#).



ICMEs and thus the interaction process. The present study is limited because of the lack of composition observations of the ICMEs before the interaction phase. The composition observations of the interacting ICMEs from the multi-spacecraft at different heliocentric distances, in particular before and after the interaction, will be useful in understanding the plasma processes involved in altering the composition.

Data availability statement

The original contributions presented in the study are included in the article/Supplementary Material. Further inquiries can be directed to the corresponding author.

Author contributions

NS and WM contributed to the initial conception of the paper. The analysis was carried out primarily by ZM under the guidance of NS. The main draft was prepared by NS, WM, and ZM. All of the authors have read the paper and approved its final version.

Funding

This work and the authors are supported by the India–Uzbekistan joint projects INT-UZBEK/P-15 and UZB-IND-2021-95. The major part of the work was carried out during the visit of ZM to Udaipur Solar Observatory, Udaipur, in May 2022. The visit was funded by the project grant.

Acknowledgments

We use cookies

Our website uses cookies that are essential for its operation and additional cookies to track performance, or to improve and personalize our services. To manage your cookie preferences, please click Cookie Settings. For more information on how we use cookies, please see our [Cookie Policy](#).

Publisher's note

All claims expressed in this article are solely those of the authors and do not necessarily represent those of their affiliated organizations, or those of the publisher, the editors, and the reviewers. Any product that may be evaluated in this article, or claim that may be made by its manufacturer, is not guaranteed or endorsed by the publisher.

References

Burlaga, L. F., Plunkett, S. P., and Cyr, St.O. C. (2002). Successive CMEs and complex ejecta. *J. Geophys. Res. Space Phys.* 107, 1266.
doi:10.1029/2001JA000255

[CrossRef Full Text](#) | [Google Scholar](#)

Burlaga, L., Sittler, E., Mariani, F., and Schwenn, R. (1981). Magnetic loop behind an interplanetary shock: Voyager, Helios, and IMP 8 observations. *J. Geophys. Res. Space Phys.* 86, 6673–6684.
doi:10.1029/JA086iA08p06673

[CrossRef Full Text](#) | [Google Scholar](#)

Cane, H. V., and Richardson, I. G. (2003). Interplanetary coronal mass ejections in the near-Earth solar wind during 1996–2002. *J. Geophys. Res. Space Phys.* 108, 1156.
doi:10.1029/2002JA009817

[CrossRef Full Text](#) | [Google Scholar](#)

Chertok, I. M., Grechnev, V. V., Hudson, H. S., and Nitta, N. V. (2004). Homologous large-scale

We use cookies

Our website uses cookies that are essential for its operation and additional cookies to track performance, or to improve and personalize our services. To manage your cookie preferences, please click Cookie Settings. For more information on how we use cookies, please see our [Cookie Policy](#).

[CrossRef Full Text](#) | [Google Scholar](#)

Elliott, H. A., McComas, D. J., Schwadron, N. A.,
Gosling, J. T., Skoug, R. M., Gloeckler, G., et al.
(2005). An improved expected temperature
formula for identifying interplanetary coronal mass
ejections. *J. Geophys. Res. Space Phys.* 110,
A04103. doi:10.1029/2004JA010794

[CrossRef Full Text](#) | [Google Scholar](#)

Farrugia, C., and Berdichevsky, D. (2004).
Evolutionary signatures in complex ejecta and
their driven shocks. *Ann. Geophys.* 22, 3679–3698.
doi:10.5194/angeo-22-3679-2004

[CrossRef Full Text](#) | [Google Scholar](#)

Farrugia, C. J., Jordanova, V. K., Thomsen, M. F.,
Lu, G., Cowley, S. W. H., and Ogilvie, K. W. (2006).
A two-ejecta event associated with a two-step
geomagnetic storm. *J. Geophys. Res. Space
Phys.* 111, A11104. doi:10.1029/2006JA011893

[CrossRef Full Text](#) | [Google Scholar](#)

Feldman, U., Landi, E., and Schwadron, N. A.
(2005). On the sources of fast and slow solar wind.
J. Geophys. Res. Space Phys. 110, A07109.
doi:10.1029/2004JA010918

[CrossRef Full Text](#) | [Google Scholar](#)

Fisk, L. A., Schwadron, N. A., and Zurbuchen, T. H.
(1998). On the slow solar wind. *Space Sci. Rev.* 86,
51–60. doi:10.1023/A:1005015527146

[CrossRef Full Text](#) | [Google Scholar](#)

We use cookies

Our website uses cookies that are essential for
its operation and additional cookies to track
performance, or to improve and personalize our
services. To manage your cookie preferences,
please click Cookie Settings. For more
information on how we use cookies, please see
our [Cookie Policy](#)

Connection of enhanced heavy ion charge states
in the interplanetary medium: Implications for the
flux-rope structure of CMEs. *Sol. Phys.* 284, 17–46.
doi:10.1007/s11207-012-0215-2

[CrossRef Full Text](#) | [Google Scholar](#)

Gopalswamy, N., Mikić, Z., Maia, D., Alexander, D., Cremades, H., Kaufmann, P., et al. (2006). The pre-CME sun. *Space Sci. Rev.* 123, 303–339.
doi:10.1007/s11214-006-9020-2

[CrossRef Full Text](#) | [Google Scholar](#)

Gopalswamy, N. (2006). Properties of interplanetary coronal mass ejections. *Space Sci. Rev.* 124, 145–168. doi:10.1007/s11214-006-9102-1

[CrossRef Full Text](#) | [Google Scholar](#)

Gopalswamy, N., Xie, H., Yashiro, S., and Usoskin, I. (2005). "Coronal mass ejections and ground level enhancements," in *29th international cosmic ray conference (ICRC29)*. Editors B. S. Acharya, S. Gupta, P. Jagadeesan, J. Jain, S. Karthikeyan, S. Morisset al. (Tata Institute of Fundamental Research), 169–172.

[Google Scholar](#)

Gruesbeck, J. R., Lepri, S. T., Zurbuchen, T. H., and Antiochos, S. K. (2011). Constraints on coronal mass ejection evolution from *in situ* observations of ionic charge states. *Astrophysical J.* 730, 103.
doi:10.1088/0004-637X/730/2/103

[CrossRef Full Text](#) | [Google Scholar](#)

We use cookies

Our website uses cookies that are essential for its operation and additional cookies to track performance, or to improve and personalize our services. To manage your cookie preferences, please click Cookie Settings. For more information on how we use cookies, please see our [Cookie Policy](#).

[CrossRef Full Text](#) | [Google Scholar](#)

Huang, J., Liu, Y. C. M., Peng, J., Qi, Z., Li, H., Klecker, B., et al. (2018). The distributions of iron average charge states in small flux ropes in interplanetary space: Clues to their twisted structures. *J. Geophys. Res. Space Phys.* 123, 7167–7180. doi:10.1029/2018JA025660

[CrossRef Full Text](#) | [Google Scholar](#)

Hundhausen, A. J., Gilbert, H. E., and Bame, S. J. (1968). The state of ionization of oxygen in the solar wind. *Astrophysical J.* 152, L3. doi:10.1086/180165

[CrossRef Full Text](#) | [Google Scholar](#)

Huttunen, K. E. J., Schwenn, R., Bothmer, V., and Koskinen, H. E. J. (2005). Properties and geoeffectiveness of magnetic clouds in the rising, maximum and early declining phases of solar cycle 23. *Ann. Geophys.* 23, 625–641. doi:10.5194/angeo-23-625-2005

[CrossRef Full Text](#) | [Google Scholar](#)

Kienreich, I. W., Veronig, A. M., Muhr, N., Temmer, M., Vršnak, B., and Nitta, N. (2011). Case study of four homologous large-scale coronal waves observed on 2010 April 28 and 29. *Astrophysical J. Lett.* 727, L43. doi:10.1088/2041-8205/727/2/L43

[CrossRef Full Text](#) | [Google Scholar](#)

Kilpua, E. K. J., Good, S. W., Palmerio, E., Asvestari, E., Lummo, E., Ala-Lahти, M., et al. (2019)

We use cookies

Our website uses cookies that are essential for its operation and additional cookies to track performance, or to improve and personalize our services. To manage your cookie preferences, please click Cookie Settings. For more information on how we use cookies, please see our [Cookie Policy](#).

[CrossRef Full Text](#) | [Google Scholar](#)

Kilpua, E., Koskinen, H. E. J., and Pulkkinen, T. I. (2017). Coronal mass ejections and their sheath regions in interplanetary space. *Living Rev. Sol. Phys.* 14, 5. doi:10.1007/s41116-017-0009-6

[PubMed Abstract](#) | [CrossRef Full Text](#) | [Google Scholar](#)

Laming, J. M. (2015). The FIP and inverse FIP effects in solar and stellar coronae. *Living Rev. Sol. Phys.* 12, 2. doi:10.1007/lrsp-2015-2

[CrossRef Full Text](#) | [Google Scholar](#)

Lepping, R. P., Burlaga, L. F., Szabo, A., Ogilvie, K. W., Mish, W. H., Vassiliadis, D., et al. (1997). The Wind magnetic cloud and events of October 18–20, 1995: Interplanetary properties and as triggers for geomagnetic activity. *J. Geophys. Res. Space Phys.* 102, 14049–14063. doi:10.1029/97JA00272

[CrossRef Full Text](#) | [Google Scholar](#)

Lepri, S. T., Zurbuchen, T. H., Fisk, L. A., Richardson, I. G., Cane, H. V., and Gloeckler, G. (2001). Iron charge distribution as an identifier of interplanetary coronal mass ejections. *J. Geophys. Res. Space Phys.* 106, 29231–29238. doi:10.1029/2001JA000014

[CrossRef Full Text](#) | [Google Scholar](#)

Li, T., and Zhang, J. (2013). Homologous flux ropes observed by the solar dynamics observatory atmospheric imaging assembly. *Astrophysical J.*

We use cookies

Our website uses cookies that are essential for its operation and additional cookies to track performance, or to improve and personalize our services. To manage your cookie preferences, please click Cookie Settings. For more information on how we use cookies, please see our [Cookie Policy](#).

[Articles](#)[Research Topics](#)[Editorial board](#)

Lugaz, N., and Farrugia, C. J. (2014). A new class of complex ejecta resulting from the interaction of two CMEs and its expected geoeffectiveness. *Geophys. Res. Lett.* 41, 769–776. doi:10.1002/2013GL058789

[CrossRef Full Text](#) | [Google Scholar](#)

Lugaz, N., Farrugia, C. J., Manchester, W., and Schwadron, N. (2013). The interaction of two coronal mass ejections: Influence of relative orientation. *Astrophysical J.* 778, 20. doi:10.1088/0004-637X/778/1/20

[CrossRef Full Text](#) | [Google Scholar](#)

Lugaz, N., Farrugia, C. J., Smith, C. W., and Paulson, K. (2015). Shocks inside CMEs: A survey of properties from 1997 to 2006. *J. Geophys. Res. Space Phys.* 120, 2409–2427. doi:10.1002/2014JA020848

[CrossRef Full Text](#) | [Google Scholar](#)

Lugaz, N., Farrugia, C. J., Winslow, R. M., Al-Haddad, N., Kilpua, E. K. J., and Riley, P. (2016). Factors affecting the geoeffectiveness of shocks and sheaths at 1 AU. *J. Geophys. Res. Space Phys.* 121 (10), 10861–10879. doi:10.1002/2016JA023100

[PubMed Abstract](#) | [CrossRef Full Text](#) | [Google Scholar](#)

Lugaz, N., Manchester, W., and Gombosi, T. I. (2005). Numerical simulation of the interaction of two coronal mass ejections from sun to Earth. *Astrophysical J.* 634, 651–662. doi:10.1086/491782

We use cookies

Our website uses cookies that are essential for its operation and additional cookies to track performance, or to improve and personalize our services. To manage your cookie preferences, please click Cookie Settings. For more information on how we use cookies, please see our [Cookie Policy](#).

[Articles](#)[Research Topics](#)[Editorial board](#)

COMPOSITION STRUCTURE OF CORONAL MASS EJECTIONS
in axisymmetric magnetohydrodynamic models.
Astrophysical J. 740, 112. doi:10.1088/0004-
637X/740/2/112

[CrossRef Full Text](#) | [Google Scholar](#)

Manchester, W., Kilpua, E. K. J., Liu, Y. D., Lugaz, N.,
Riley, P., Török, T., et al. (2017). The physical
processes of CME/ICME evolution. *Space Sci.
Rev.* 212, 1159–1219. doi:10.1007/s11214-017-
0394-0

[CrossRef Full Text](#) | [Google Scholar](#)

Mishra, W., Srivastava, N., and Chakrabarty, D.
(2015a). Evolution and consequences of
interacting CMEs of 9 - 10 november 2012 using
STEREO/SECCHI and *in situ* observations. *Sol.
Phys.* 290, 527–552. doi:10.1007/s11207-014-
0625-4

[CrossRef Full Text](#) | [Google Scholar](#)

Mishra, W., and Srivastava, N. (2013). Estimating
the arrival time of earth-directed coronal mass
ejections at *in situ* spacecraft using COR and HI
observations from STEREO. *Astrophysical J.* 772,
70. doi:10.1088/0004-637X/772/1/70

[CrossRef Full Text](#) | [Google Scholar](#)

Mishra, W., and Srivastava, N. (2014).
Morphological and kinematic evolution of three
interacting coronal mass ejections of 2011
february 13-15. *Astrophysical J.* 794, 64.
doi:10.1088/0004-637X/794/1/64

[CrossRef Full Text](#) | [Google Scholar](#)

We use cookies

Our website uses cookies that are essential for
its operation and additional cookies to track
performance, or to improve and personalize our
services. To manage your cookie preferences,
please click Cookie Settings. For more
information on how we use cookies, please see
our [Cookie Policy](#)

[CrossRef Full Text](#) | [Google Scholar](#)

Mishra, W., Wang, Y., Srivastava, N., and Shen, C. (2017). Assessing the nature of collisions of coronal mass ejections in the inner heliosphere. *Astrophysical J. Suppl. Ser.* 232, 5. doi:10.3847/1538-4365/aa8139

[CrossRef Full Text](#) | [Google Scholar](#)

Owens, M. J. (2018). Solar wind and heavy ion properties of interplanetary coronal mass ejections. *Sol. Phys.* 293, 122. doi:10.1007/s11207-018-1343-0

[CrossRef Full Text](#) | [Google Scholar](#)

Palmerio, E., Kilpua, E. K. J., Witasse, O., Barnes, D., Sánchez-Cano, B., Weiss, A. J., et al. (2021). CME magnetic structure and IMF preconditioning affecting SEP transport. *Space19*, e2020SW002654. doi:10.1029/2020SW002654

[CrossRef Full Text](#) | [Google Scholar](#)

Rakowski, C. E., Laming, J. M., and Lepri, S. T. (2007). Ion charge states in halo coronal mass ejections: What can we learn about the explosion? *Astrophysical J.* 667, 602–609. doi:10.1086/520914

[CrossRef Full Text](#) | [Google Scholar](#)

Reinard, A. A. (2008). Analysis of interplanetary coronal mass ejection parameters as a function of energetics, source location, and magnetic structure. *Astrophysical J.* 682, 1289–1305. doi:10.1086/589322

We use cookies

Our website uses cookies that are essential for its operation and additional cookies to track performance, or to improve and personalize our services. To manage your cookie preferences, please click Cookie Settings. For more information on how we use cookies, please see our [Cookie Policy](#).



ejections at 1 AU using multiple solar-wind plasma
composition anomalies. *J. Geophys. Res. Space
Phys.* 109, A09104. doi:10.1029/2004JA010598

[CrossRef Full Text](#) | [Google Scholar](#)

Richardson, I. G., and Cane, H. V. (2010). Near-earth interplanetary coronal mass ejections during solar cycle 23 (1996 - 2009): Catalog and summary of properties. *Sol. Phys.* 264, 189–237. doi:10.1007/s11207-010-9568-6

[CrossRef Full Text](#) | [Google Scholar](#)

Rodkin, D., Goryaev, F., Pagano, P., Gibb, G., Slemzin, V., Shugay, Y., et al. (2017). Origin and ion charge state evolution of solar wind transients during 4 - 7 august 2011. *Sol. Phys.* 292, 90. doi:10.1007/s11207-017-1109-0

[CrossRef Full Text](#) | [Google Scholar](#)

Rodkin, D., Slemzin, V., Zhukov, A. N., Goryaev, F., Shugay, Y., and Veselovsky, I. (2018). Single ICMEs and complex transient structures in the solar wind in 2010 - 2011. *Sol. Phys.* 293, 78. doi:10.1007/s11207-018-1295-4

[CrossRef Full Text](#) | [Google Scholar](#)

Schmidt, J., and Cargill, P. (2004). A numerical study of two interacting coronal mass ejections. *Ann. Geophys.* 22, 2245–2254. doi:10.5194/angeo-22-2245-2004

[CrossRef Full Text](#) | [Google Scholar](#)

Shen, F., Wang, Y., Shen, C., and Feng, X. (2017). On the collision nature of two coronal mass

We use cookies

Our website uses cookies that are essential for its operation and additional cookies to track performance, or to improve and personalize our services. To manage your cookie preferences, please click Cookie Settings. For more information on how we use cookies, please see our [Cookie Policy](#).

[Articles](#)[Research Topics](#)[Editorial board](#)

Song, H. Q., Zhong, J., Chen, Y., Cheng, X., Li, G., and Wang, Y. M. (2015b). First taste of hot channel in interplanetary space. *Astrophysical J.* 803, 96. doi:10.1088/0004-637X/803/2/96

[CrossRef Full Text](#) | [Google Scholar](#)

Song, H. Q., Zhong, Z., Chen, Y., Zhang, J., Cheng, X., Zhao, L., et al. (2016). A statistical study of the average iron charge state distributions inside magnetic clouds for solar cycle 23. *Astrophysical J. Suppl. Ser.* 224, 27. doi:10.3847/0067-0049/224/2/27

[CrossRef Full Text](#) | [Google Scholar](#)

Srivastava, N., Mishra, W., and Chakrabarty, D. (2018). Interplanetary and geomagnetic consequences of interacting CMEs of 13 - 14 June 2012. *Sol. Phys.* 293, 5. doi:10.1007/s11207-017-1227-8

[CrossRef Full Text](#) | [Google Scholar](#)

St. Cyr, O. C., Plunkett, S. P., Michels, D. J., Paswaters, S. E., Koomen, M. J., Simnett, G. M., et al. (2000). Properties of coronal mass ejections: SOHO LASCO observations from january 1996 to June 1998. *J. Geophys. Res. Space Phys.* 105, 18169–18186. doi:10.1029/1999JA000381

[CrossRef Full Text](#) | [Google Scholar](#)

Stone, E. C., Frandsen, A. M., Mewaldt, R. A., Christian, E. R., Margolies, D., Ormes, J. F., et al. (1998). The advanced composition explorer. *Space Sci. Rev.* 86, 1–22. doi:10.1023/A:1005082526237

[CrossRef Full Text](#) | [Google Scholar](#)

We use cookies

Our website uses cookies that are essential for its operation and additional cookies to track performance, or to improve and personalize our services. To manage your cookie preferences, please click Cookie Settings. For more information on how we use cookies, please see our [Cookie Policy](#).

[Articles](#)[Research Topics](#)[Editorial board](#)[Interaction process for the events from 2011](#)february 14-15. *Astrophysical J.* 785, 85.

doi:10.1088/0004-637X/785/2/85

[CrossRef Full Text](#) | [Google Scholar](#)

von Steiger, R., and Zurbuchen, T. H. (2003). "Composition signatures of interplanetary coronal mass ejections," in *Solar variability as an input to the earth's environment*. Editor A. Wilson (ESA Publications Division), 835–840.

[Google Scholar](#)

Wang, W., Liu, R., Wang, Y., Hu, Q., Shen, C., Jiang, C., et al. (2017). Buildup of a highly twisted magnetic flux rope during a solar eruption. *Nat. Commun.* 8, 1330. doi:10.1038/s41467-017-01207-x

[PubMed Abstract](#) | [CrossRef Full Text](#) | [Google Scholar](#)

Wang, Y. M. (2012). Semiempirical models of the slow and fast solar wind. *Space Sci. Rev.* 172, 123–143. doi:10.1007/s11214-010-9733-0

[CrossRef Full Text](#) | [Google Scholar](#)

Wang, Y. M., Ye, P. Z., and Wang, S. (2003). Multiple magnetic clouds: Several examples during March–April 2001. *J. Geophys. Res. Space Phys.* 108, 1370. doi:10.1029/2003JA009850

[CrossRef Full Text](#) | [Google Scholar](#)

Webb, D. F., and Howard, T. A. (2012). Coronal mass ejections: Observations. *Living Rev. Sol. Phys.* 9, doi:10.12012/lrsp-2012-2

We use cookies

Our website uses cookies that are essential for its operation and additional cookies to track performance, or to improve and personalize our services. To manage your cookie preferences, please click Cookie Settings. For more information on how we use cookies, please see our [Cookie Policy](#).

[Articles](#)[Research Topics](#)[Editorial board](#)

TU, W., FARRUGIA, C. J., GALVAN, A. D., LUGAZ, N.,
Luhmann, J. G., Simunac, K. D. C., et al. (2016).
Small solar wind transients at 1 AU: STEREO
observations (2007–2014) and comparison with
near-earth wind results (1995–2014). *J. Geophys.
Res. Space Phys.* 121, 5005–5024.
doi:10.1002/2016JA022642

[CrossRef Full Text](#) | [Google Scholar](#)

Zhang, J., and Wang, J. (2002). Are homologous
flare-coronal mass ejection events triggered by
moving magnetic features? *Astrophysical J.* 566,
L117–L120. doi:10.1086/339660

[CrossRef Full Text](#) | [Google Scholar](#)

Zhao, L., Landi, E., Zurbuchen, T. H., Fisk, L. A., and
Lepri, S. T. (2014). The evolution of 1 AU equatorial
solar wind and its association with the
morphology of the heliospheric current sheet
from solar cycles 23 to 24. *Astrophysical J.* 793, 44.
doi:10.1088/0004-637X/793/1/44

[CrossRef Full Text](#) | [Google Scholar](#)

Zhao, L., Zurbuchen, T. H., and Fisk, L. A. (2009).
Global distribution of the solar wind during solar
cycle 23: ACE observations. *Geophys. Res. Lett.* 36,
L14104. doi:10.1029/2009GL039181

[CrossRef Full Text](#) | [Google Scholar](#)

Zurbuchen, T. H., Fisk, L. A., Lepri, S. T., and von
Steiger, R. (2003). "The composition of
interplanetary coronal mass ejections," in *Solar
wind ten: Proceedings of the tenth international
solar wind conference*. Editors M. Velli, R. Bruno, F.

We use cookies

Our website uses cookies that are essential for
its operation and additional cookies to track
performance, or to improve and personalize our
services. To manage your cookie preferences,
please click Cookie Settings. For more
information on how we use cookies, please see
our [Cookie Policy](#)



(2023). COMPOSITION OF CORONAL MASS EJECTIONS.

Astrophysical J 826, 10. doi:10.3847/0004-637X/826/1/10

[CrossRef Full Text](#) | [Google Scholar](#)

Keywords: CME–CME interaction, ICME, solar wind, compositional signatures, charge states

Citation: Srivastava N, Mirtoshev Z and Mishra W (2023) Investigating the variations in the composition and heating of interacting ICMEs. *Front. Astron. Space Sci.* 10:1154612. doi: 10.3389/fspas.2023.1154612

Received: 30 January 2023; **Accepted:** 24 April 2023;

Published: 30 May 2023.

Edited by:

[Divya Oberoi](#), Tata Institute of Fundamental Research, India

Reviewed by:

[Emilia Kilpua](#), University of Helsinki, Finland

[Giovanni Lapenta](#), KU Leuven, Belgium

Copyright © 2023 Srivastava, Mirtoshev and Mishra. This is an open-access article distributed under the terms of the [Creative Commons Attribution License \(CC BY\)](#). The use, distribution or reproduction in other forums is permitted, provided the original author(s) and the copyright owner(s) are credited and that the original publication in this journal is cited, in accordance with accepted academic practice. No use, distribution or reproduction is permitted which does not comply with these terms.

***Correspondence:** Zavkiddin Mirtoshev,

We use cookies

Our website uses cookies that are essential for its operation and additional cookies to track performance, or to improve and personalize our services. To manage your cookie preferences, please click Cookie Settings. For more information on how we use cookies, please see our [Cookie Policy](#).

Similar articles

**ORIGINAL
RESEARCH**

Published on 30 Ja

Deciphering solar magnetic activity: The (solar) hale cycle terminator of 2021

Scott W. McIntosh · Robert J. Leamon · Ricky Egeland

**ORIGINAL
RESEARCH**

Published on 01 Fe

The Highly Accurate Relation Between the Radius and Mass of the White Dwarf Star From Zero to Finite Temperature

Ting-Hang Pei

**ORIGINAL
RESEARCH**

Published on 10 Ma

Deciphering Solar Magnetic Activity: The Solar Cycle Clock

Robert J. Leamon · Scott W. McIntosh · Alan M. Title

**ORIGINAL
RESEARCH**

Published on 05 Ju

Investigating Remote-Sensing Techniques to Reveal Stealth Coronal Mass Ejections

Erika Palmerio · Nariaki V. Nitta · Tamitha Mulligan · Marilena Mierla · Jennifer O'Kane · Ian G. Richardson · Suvadip Sinha · Nandita

We use cookies

Our website uses cookies that are essential for its operation and additional cookies to track performance, or to improve and personalize our services. To manage your cookie preferences, please click Cookie Settings. For more information on how we use cookies, please see our [Cookie Policy](#).



Articles

Research Topics

Editorial board

doi
10.3389/fspas.2023.1154612

doi
10.3389/fspas.2021

doi
10.3389/fspas.2022

doi
10.3389/fspas.2021

15,513
views
22 citations

11,373
views
8 citations

9,811
views
22 citations

9,147
views
18 citations

Guidelines



Explore



Outreach



Connect



Follow us



© 2025 Frontiers Media S.A. All rights reserved

Privacy policy | Terms and conditions

We use cookies

Our website uses cookies that are essential for its operation and additional cookies to track performance, or to improve and personalize our services. To manage your cookie preferences, please click Cookie Settings. For more information on how we use cookies, please see our [Cookie Policy](#).